REVIEW

Sedimentary and palaeoenvironmental evolution of the Junggar Basin, Xinjiang, Northwest China

Weihua Bian · Jens Hornung · Zhenhua Liu ·
Pujun Wang · Matthias Hinderer

Abstract This review paper summarizes the sedimentary and palaeoenvironmental evolution of the Junggar Basin in Northwest China largely based on hardly accessible Chinese language papers, and complemented by own field observations and a critical survey of key sediment cores from petroleum wells. We have combined this information and updated existing lithofacies and isopach maps for characteristic time slices of basin evolution and palaeoenvironmental change. The Junggar Basin was initiated during the late stage of collisional tectonics in the southern Central Asian Orogenic Belt (Altaids) since the Early Permian. According to studies in surrounding mountain chains and geophysical surveys, the basement consists of a collage of oceanic basins, intraoceanic island arcs, and microcontinents of Precambrian to Palaeozoic age. The basin fill is subdivided into three tectonically controlled stratigraphic sequences which are separated by two regional angular unconformities. The first cycle in the Permian and Triassic is characterized by an Early Permian extensional strike-slip and a Late Permian to Triassic compressional foreland setting. After an Early Permian marine regression, persistent nonmarine fluvio-lacustrine conditions were established containing probably the thickest organic-rich mudstone interval in the world, which act as major source rocks of the basin. Starting with four depocenters, the basin was unified during the Triassic. The preserved total maximum thickness of this cycle is about 8,500 m in the southern depocenter. During the second intracontinental depression cycle, subsidence slowed down and the depocenter migrated towards the basin center reaching a maximum thickness of 6,000 m. The palaeoenvironment was dominated by a large oscillating freshwater lake receiving changing quantities of clastic sediments from the surrounding mountain ranges and forming alluvial fans, braid plains, and deltas partly containing coal seams of economic interest. Sedimentary facies, pollen, and palaeobotanical plant fossils show an overall aridization trend and a shrinking lake cover. During the Neogene cycle, the depocenter migrated back to the south and the former asymmetric foreland basin was reactivated due to thrusting and rapid uplift of the Tian Shan. The maximum thickness of these molasse-type deposits exceeds 5,000 m. Despite its strong potential, there is still a lack of high resolution bio- and cyclostratigraphy, sequence stratigraphy, and palaeoclimate studies in the Junggar Basin to elucidate local versus regional palaeoenvironmental patterns and to better constrain far-distance tectonic forcing.

W.-H. Bian · J. Hornung · M. Hinderer (✉)
Institut für Angewandte Geowissenschaften,
Technische Universität Darmstadt,
Schnittspahnstraße 9,
Darmstadt 64287, Germany
e-mail: hinderer@geo.tu-darmstadt.de

W.-H. Bian · P.-J. Wang
College of Earth Sciences, Jilin University,
2199 Jianshe Street,
Changchun 130061, China

Z.-H. Liu
Northwest Branch, Research Institute of Petroleum Exploration and Development (RIPED),
PetroChina, China

Introduction

The Junggar Basin in the Xinjiang Uygur Autonomous Region of Northwest China is one of the most prominent walled sedimentary basins in western China, surrounded by active mountain ranges but with little internal deformation and an exceptionally long history of subsidence and impoundment of sediments (Carroll et al. 2010). These basins developed since the Late Palaeozoic after amalgamation of microcontinents, ocean basins, and island arcs forming the Altaid orogenic belt, also called the Central Asian Orogenic Belt (CAOB) which represents the largest crustal growth in Palaeozoic time (Sengör et al. 1993). The sedimentary fill is nonmarine and dominated by fluvio-lacustrine sandstones and mudstones. Most basins were repeatedly covered by large lakes and house substantial economic resources of coal, oil shale, petroleum, and evaporite minerals (Zhao et al. 2010). In addition, they preserve important palaeobiological and continental palaeoclimate records.

The Junggar Basin has a total area of 136,000 km^2 and is presently surrounded by the Zaire Mountains and Halalate Mountains to the west, the Qingelid Mountains and Karamaili Mountains to the northeast, and the east–west trending Boro Horo Mountains (Tian Shan) and Bogda Mountains to the south (Fig. 1a). The triangle-shaped basin can be subdivided into four geological units from the north to south namely the Wulungu Depression, Luliang Uplift, Central Depression and Piedmont Depression north of the Tian Shan Mountains (Fig. 1a). The maximum thickness of the basin fill since the Permian reaches 14,000 m in the south (Tang et al. 1997).

The juvenile Junggar Basin formed at the end of the Carboniferous after final collision of the combined Tarim–central Tian Shan Block with the northern Tian Shan Block by post-collisional transcurrent tectonics during the Early and Middle Permian and flexural foreland subsidence in the Late Permian when subduction terminated (Chen et al. 2002; Kuang and Qi 2006; Wang et al. 2009; Xiao et al. 2009). During the Mesozoic–Cenozoic, the Junggar Basin impounded sediments almost continuously in an intracontinental setting. The basin margins, however, have been repeatedly deformed in response to successive accretion onto the south Asian margin (Hendrix et al. 1992; Carroll et al. 1995). Since Neogene, the Junggar Basin was reactivated as a foreland basin due to the collision of the Indian plate with the Eurasian plate (Hendrix et al. 1994; Guo et al. 2006; Luo et al. 2006; De Grave et al. 2007). This multiphase basin history and its intraplate position make it difficult to cast the Junggar Basin (and other nonmarine basins across China) into traditional classification schemes that emphasize plate–boundary interactions. Therefore, different

terms have been proposed to describe the specific nature of the basin such as "broken foreland basin" (Dickinson and Snyder 1978), "collisional successor basin" (Graham et al. 1993), and "walled sedimentary basin" (Carroll et al. 2010). The latter emphasizes the long-lasting closed geomorphology of this basin type with internal drainage caused by dominantly contractional intraplate deformation and being an integral part of the growth of the Asian continent since the Permian. Aridity appears to be a necessary condition to defeat orogen-traversing rivers (Sobel et al. 2003).

Temporal and spatial discrete information on the sedimentary record of the Junggar Basin is mainly based on outcrop belts within and in front of the surrounding mountain ranges that dominantly expose sedimentary facies proximal to the source areas (Hendrix et al. 1992; Fang et al. 2006; Metcalfe et al. 2009; Hornung and Hinderer 2010). The Permian is characterized by a gradual transition from deep marine to nonmarine depositional environments. This includes the possibly thickest organic-rich mudstone interval in the world approaching 2,000 m and being the major source rocks of the basin (Lawrence 1990; Carroll et al. 1992). Through the Mesozoic up to the Palaeogene, large fluvio-lacustrine deposystems persisted over the whole basin; however, several episodes of enhanced sediment input and changes in humidity and seasonality led to strong shift of lateral facies and second to fourth order vertical cyclicity (Hendrix et al. 1992; Zhao et al. 2010; Fig. 1c). In the Neogene, the southern part of the Junggar Basin experienced rapid subsidence and strong sediment supply by the rising Tian Shan converting the basin into the present asymmetric foreland basin dominated by coarse-grained molasse deposition (Chen et al. 2002; Zhang et al. 1999a; Fig. 1b).

The aim of our paper is to complement recent large-scale reviews about the Late Palaezoic to Cenozoic tectonic evolution and basin formation of northern China (Xiao et al. 2009; Carroll et al. 2010) by a review of extensive data from petroleum exploration within the Junggar Basin, that are documented only in relatively inaccessible Chinese language publications or internal reports, and compare the results with the international literature. Benefiting from geophysical exploration and petroleum drillings, more and more information about the sedimentary accumulation and basin evolution was obtained (e.g. Chen et al. 2002; He et al. 2005; Luo et al. 2006; Song 2006; Zou et al. 2007; Feng et al. 2008; Kang 2008; Liu et al. 2008; Qu et al. 2008; Zhu et al. 2008; Wu et al. 2009). In particular, we collected well information from the Xinjiang Oilfield Company including cutting logs of 150 wells and a stratigraphic framework of 520 wells and revised existing facies maps. Detailed studies on key wells acted as a control of these generalized facies maps and helped to better interpret palaeoenvironments.
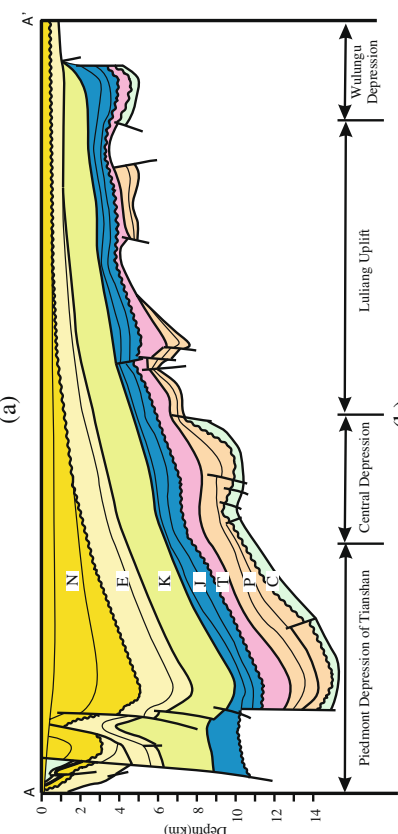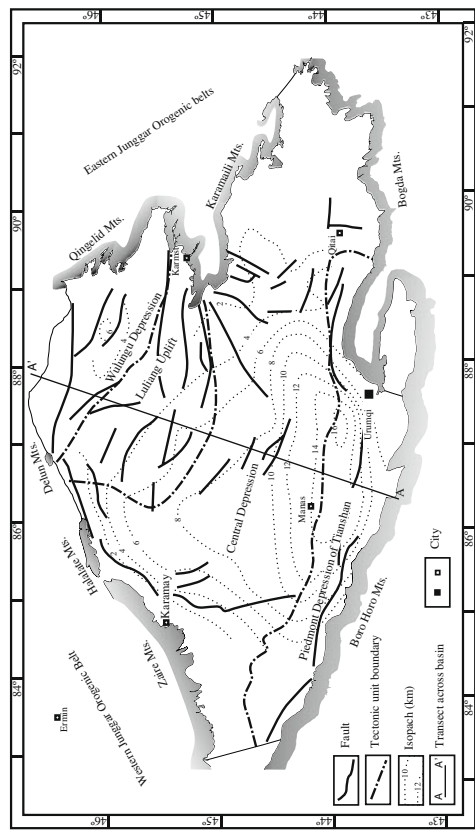
Fig. 1 Geological structure and stratigraphic framework of the Junggar Basin. a Simplified geological map (isopach data after Tang et al. 1997, fault systems and tectonic units after Xu et al. 2004). b South–north geological transect (modified after Song 2006). c Lithological section and biostratigraphic zones (formation thickness after Liu et al. 2006)

Basement of the Junggar Basin

The thick sedimentary sequence of the Junggar Basin is underlain by a pre-Carboniferous basement. There is no common idea of the basement nature yet, because direct evidence is lacking. The oldest strata discovered by petroleum wells are of Carboniferous age. Hypotheses regarding its nature include a Precambrian consolidated microcontinent with Palaeozoic strata (Zhang et al. 1993), a trapped Palaeozoic oceanic crust and arc complex (Carroll et al. 1990), and post-collisional underplated mantle-derived basic/ultrabasic rocks (Han et al. 1999). In general, structural relationships between the surrounding mountain ranges and the basin makes it likely that at least parts of the basin are underlain by similar rocks, which imply an accretionary collage of oceanic rocks and island arcs that stabilized as late as in the Late Permian (Xiao et al. 2009). In contrast to a single magmatic arc model of the 1990s (e.g., Sengör et al. 1993), the picture of archipelago-type multi-phase accretion of various arcs, marginal basins, and several microcontinental blocks have appeared and oceanic closure between the Siberian plate in the north and the Tarim and North China Block in the south progressed in a scissor-like manner from west to east (Xiao et al. 2009).

New geophysical data and isotopic dating in surrounding mountain ranges favour the microcontinent hypothesis (Qu et al. 2008; Zhang et al. 2004; Zhao et al. 2008). These authors present evidence that the pre-Carboniferous basement is of dual-layer type being composed of a Precambrian crystalline basement and a Palaeozoic basement. According to an aeromagnetic anomaly and seismic sections along Ermin-Qitai in the south and along Karamay-Karmst in the north, the presumed Precambrian crystalline basement is located in the middle-lower crust like a plate (Zhang et al. 2004). According to outcrop studies of the surrounding mountain ranges, the presumed Precambrian basement is mainly composed of granitoids with intercalated greenstones or ophiolites (Zhao et al. 2008). Radiometric dating of zircons from granitoid rocks give a maximum age of 1,908 Ma (Zhang et al. 1999b). Granites from the western Junggar Basin and ophiolites from the Luliang uplift (Fig. 1a) yielded Sm-Nd ages of 1,300–1,400 Ma (Chen et al. 2002). According to the geophysical exploration results, the current burial depth of the crystalline basement measures around 20–28 km (He et al. 2005).

The upper seismic unit of the basement is interpreted as folded Palaeozoic sediments, metamorphic rocks, volcanic rocks and intrusives ranging in age from the Cambrian to the Carboniferous. The thickness reaches about 8,000–10,000 m in the north and decreases gradually to 0–1,000 m in the southern part. Its burial depth measures about 6,000–16,000 m (He et al. 2005). There exist two generations of volcanic rocks and intrusives: (1) Lower Palaeozoic basic intrusives ("Caledonian"), and (2) Devonian to Carboniferous basic intrusives and basic to intermediate volcanic rocks ("Hercynian"; Fig. 2). This association of Palaeozoic magmatic rocks may be interpreted as a collage of intra-oceanic island arcs, oceanic basins, and microcontinents (Xiao et al. 2009).

Sedimentary fill of the Junggar Basin

According to the preferred stratigraphical framework of the Xinjiang Oil Field Company, the post-accretionary sequence of the Junggar Basin is subdivided into 23 lithostratigraphical formations with a maximum total thickness of around 14,000 m (Fig. 1c). Because all well data are referring to this stratigraphic framework and this paper aims to give a large-scale overview, we follow its

Fig. 2 Tentative map of basement lithology of the Junggar Basin (after Zhang et al. 1993)
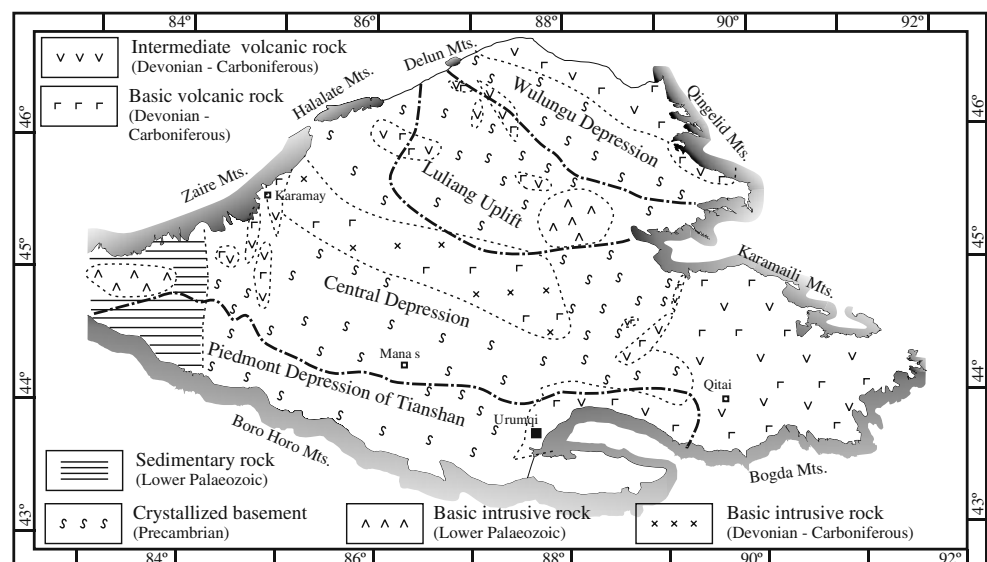
nomenclature and abbreviations. For marginal sedimentary facies in the outcrop belt, some additional or alternative terminologies are defined and used in the literature which will be not further considered here. Chronostratigraphic correlations are based on palynological biostratigraphy, but are still tentative (Fig. 1c; Hu et al. 1997; Yang et al. 2005; Luo et al. 2007; Yang et al. 2008). Recent high-resolution studies on palynomorphs showed that chronostratigraphic boundaries may shift up to hundreds of meters in the sedimentary sequence according to new data (e.g. Ashraf et al. 2010, this issue).

Below, we present a combined set of seven lithofacies and isopach maps for the Junggar Basin, based on mostly unpublished well data of Xinjiang Oil Field Company. Those wells are marked on the maps, which we have examined by own surveys of sediment cores and cuttings. A total of eight fundamental lithofacies associations have been identified according to their grain size, colour, fossil content, and architecture and grouped into (1) shallow marine carbonates, (2) lagoon (mudstones and evaporites), (3) alluvial fan (conglomerate and sandstone), (4) braided river and braid delta (conglomerate, sandstone, and coal), (5) fan delta (conglomerate and sandstone), (6) lacustrine delta (sandstone and coal), (7) lacustrine siltstones (shallow lake), and (8) lacustrine mudstone (moderately deep lake). The time slices of lithofacies and isopach maps are selected according to the three major cycles of post-accretionary tectonic evolution of the Junggar Basin again following the terminology of Xinjiang Oil Field Company (Fig. 1c): (1) foreland basin cycle from Permian to Triassic, (2) intracontinental depression basin cycle from Jurassic to Palaeogene, and (3) reactivated foreland basin cycle in the Neogene.

In detail, basin evolution was more complex and also includes transitional stages. In the lower Permian, extension with distinct subbasins and distributed depocenters dominated most probably due to transtension caused by sinistral shear within the southern Altaids (Allen et al. 1995). A sedimentary break marks the transition to Late Permian compressional tectonics and conversion in an asymmetric foreland basin north of the ancient Tian Shan. Upper Permian to Triassic deposits are lacking or are only thinly developed in the northern Junggar Basin (Fig. 1b). Although the cause of this tectonic change is not completely clear (Yang et al. 2009), the timing corresponds well to the model of Xiao et al. (2009) who concluded that subduction and orogenesis in the southern Tian Shan did not terminate before the late Permian. This "Permian–Triassic termination model" is based on subduction-related volcanic and plutonic rocks and Upper Permian radiolarites being incorporated in accretionary wedges. In this model, Early Permian strike-slip faults are interpreted as synorogenetic. Because direct evidence for a Late Permian suture

zone in the Tian Shan is missing, the authors hypothesize that this suture was subducted at the southern edge of the Tian Shan during strong Neogene compression.

The second cycle is called an intracratonic depression basin in the Chinese literature (e.g., Zhao et al. 2010) which corresponds to an intracontinental (flexural or sag) basin according to the international classification of Busby and Ingersoll (1995). During this stage, the whole basin subsided uniformly at relatively low rates. However, several episodes of enhanced sediment supply and accelerated subsidence rates are obvious, which may be attributed to far-distance stresses of accretionary processes farther south (Hendrix et al. 1992). Finally, the India–Asia collision reactivated the ancient Tian Shan and its adjacent foreland basins to the north and the south (Tarim Basin). During this third cycle of basin evolution, strongly asymmetric subsidence established with a depocenter in the southern Junggar Basin of up to 5,000 m thickness in front of the Tian Shan (Fig. 1c).

Foreland basin cycle (Permian to Triassic)

Eastward progressing closure and compression of the southern Altaids together with the formation of isolated strike-slip basins led to an ultimate retrogradation of marine conditions in the late Early Permian which were limited to the southeastern part of the Junggar Basin and are also documented at the margins of the Turpan-Hami Basin (Liu 1989; Shao et al. 1999). There are three depocentres during the Early Permian. One depocentre is located in the northwest (Fig. 3). It shows a preserved thickness of more than 4,000 m dominated by fine shallow lake sediments. A few alluvial fans formed along the northwestern margin. They are mainly composed of coarse debris and volcanic materials due to the persistent strong volcanic activities (Huang 1999; Kuang et al. 2008). Another depocentre is located in the foreland depression of the Tian Shan (Fig. 3). The preserved sedimentary thickness also measures more than 4,000 m. The main portions are fine grained sediments (clay and silt) and a minor share of evaporites which had accumulated in lagoons. The basin fill shows an asymmetric pattern with a northward decrease of the sedimentary thickness. Shallow marine deposits occur near Urumqi with a thickness of more than 2,000 m. They are chiefly composed of silt, sand and carbonate. Another depocentre is situated in the northeastern margin and close to the Karamaili Mountains. The preserved thickness is less than 1,000 m. The lithofacies is similar to the northwestern depocentre which is composed of clay and silt. The main sediment flux occurred from the northwest and south (Fig. 3).

At the end of the Permian, complete nonmarine sedimentation has established and shallow lake deposits accumulated basinwide. Alluvial fans shedded sediments from the Halalate Mountains in the northwest (Zou et al. 2007) (Fig. 4). A new asymmetric subbasin, Wulungu

Fig. 3 Lithofacies distribution in the Junggar Basin during the Early Permian (modified after Mou et al. 1992; Yan et al. 2009; Zhang et al. 1993) and isopach map of the Lower Permian (P₁) (modified after Tian 1989)
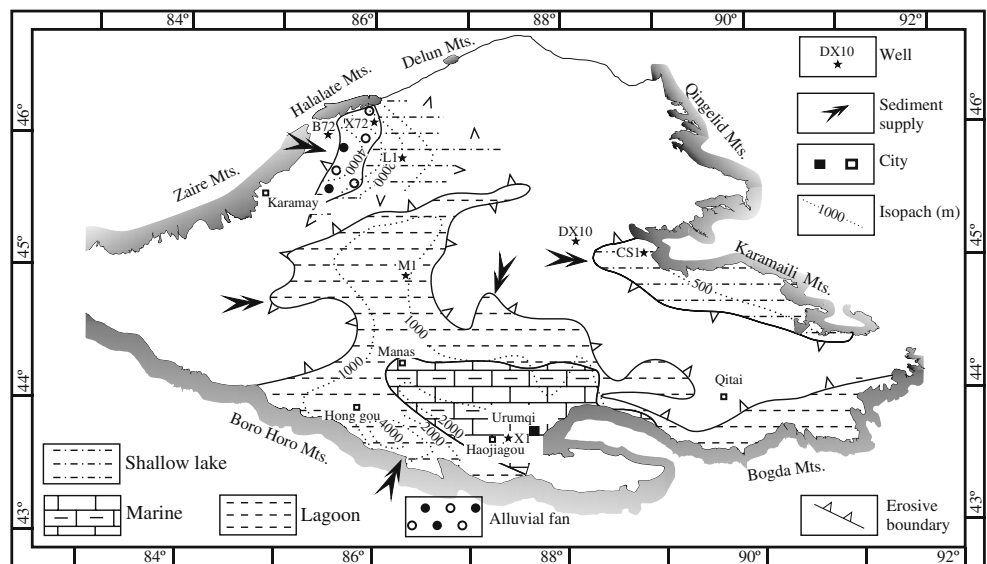
subbasin, formed close to the Qingelid Mountains (Figs. 1a and 4) where the preserved deposits are mainly composed of clay and silt with a thickness of about 1,000 m. The most prominent depocentre was established between Manas and Urumqi with a sediment thickness of more than 4,500 m. The main sediment supply was from the northwest and south (Fig. 4).

During the Early-Middle Triassic, the previously isolated subbasins were integrated to build up a shallow unified basin covered by a large lake which increased in depth during the Triassic (Fig. 5). Alluvial fan and delta systems of various scales formed around the basin indicating an increasing supply of clastic sediments from the surrounding mountain ranges. The clastic sediments show reddish colours before they change to greyish in the Upper Triassic. The rising lake level led to a retrogradation of alluvial fan and delta systems during the Late Triassic and the

deposition of the first coal seams (Yu et al. 2005). Delta systems formed along the northern and southern margins consisting of dark fine debris (silt and fine-grained sand). At the stationary depocentre near Urumqi, Triassic deposits reach a maximum thickness of more than 2,800 m. Most sediments were derived from the south and north. At the end of Triassic, deposits covered much more of the region than the present Junggar Basin does before the basin was elevated and the upper Triassic had undergone erosion, which terminated the foreland basin cycle.

Intracontinental depression cycle (Jurassic to Palaeogene)

After a Triassic/Jurassic unconformity over most parts of the basin, almost the whole basin was covered with braid-delta deposits except for three shallow lakes with silt deposition and one moderately deep lake with deposition of

Fig. 4 Lithofacies distribution in the Junggar Basin during the Middle-Late Permian (modified after Mou et al. 1992; Zhang et al. 1993) and isopach map of the Middle-Upper Permian (P₂₊₃) (modified after Tian 1989)
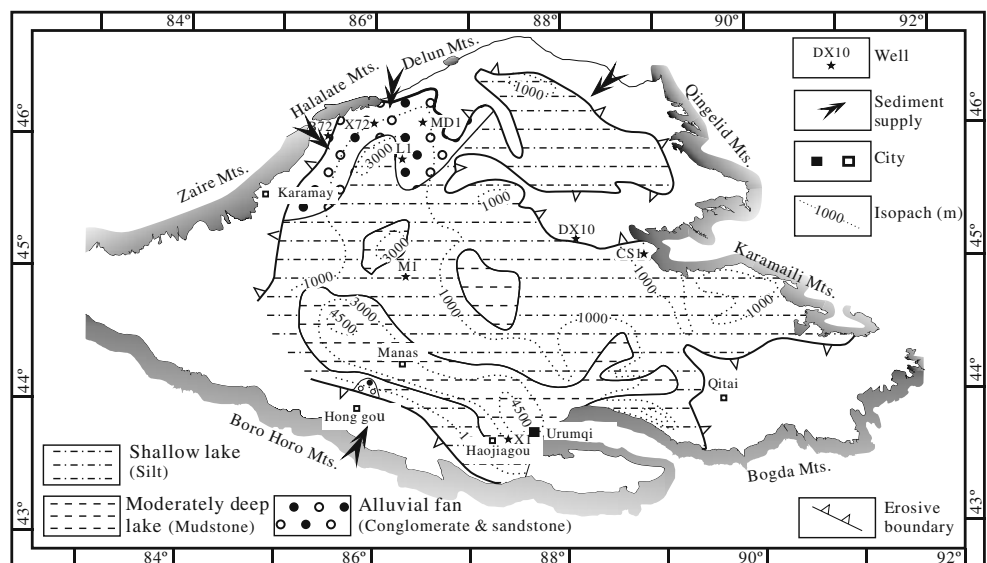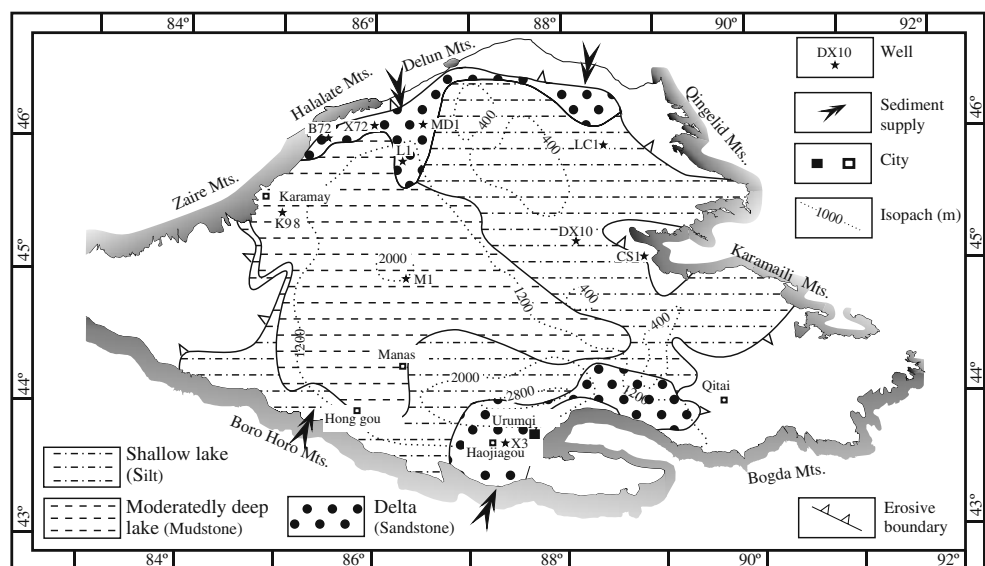
Fig. 5 Lithofacies distribution in the Junggar Basin during the Late Triassic (modified after Zhang et al. 1993) and isopach map for the whole Triassic (T) (modified after Tian 1989)

mud in the southern central part of the basin (Fig. 6). This tectonic episode is contemporaneous with the separation of the Turpan-Hami Basin in the southwest due to the uplift and exhumation of the Bogda Shan Mountain range (Shao et al. 2001; Greene et al. 2005). Hendrix et al. (1992) relates this compressional episode to the collision of the Qiantang Block at the southern margin of the Tarim Block.

During the Early to Middle Jurassic, braid-delta systems entered the perennial large and oscillating freshwater lake from the northern and southern basin margins (Liu et al. 2008) forming huge coal seams (Ding et al. 1996; He et al. 2004; Zhu et al. 2002). The strata were almost horizontal or with tiny dip angles. The subsidence rate increased to the south from 20 to 120 m/Ma (Wang et al. 2007). The lithology of the Jurassic is mostly composed of clay and fine sandstone except for the basal part which is dominated by sandstones and conglomerates (Fig. 1c). A depocentre developed

between Manas and Urumqi with the maximum preserved thickness of more than 4,000 m. The main sediment supply is from north and south (Hu et al. 2001). The Upper Jurassic in the Junggar Basin was largely eroded with significant reduction of sediment thicknesses (Wang et al. 2001).

The Lower Cretaceous deposits cover the Jurassic with local angular unconformities. The timing of this repeated tectonic episode corresponds to the collision of the Lhasa Block in the south (Hendrix et al. 1992, Hendrix 2000). Delta systems formed around the margins of the Junggar Basin (Gao et al. 2004). Most of the basin was covered with a shallow lake and in the basin centre with a moderately deep lake (Fig. 7). The main lithology consists of interbedded clay and fine sandstones. The basin's north-western margin was beyond the present Halalate Mountains (Li et al. 2009). During the later Cretaceous, the lake shrunk to the southern part of the basin and the main

Fig. 6 Lithofacies distribution in the Junggar Basin during the Early Jurassic (modified after Zhang et al. 1993; Zhu et al. 2008) and isopach map for the whole Jurassic (J) (modified after Tian 1989)
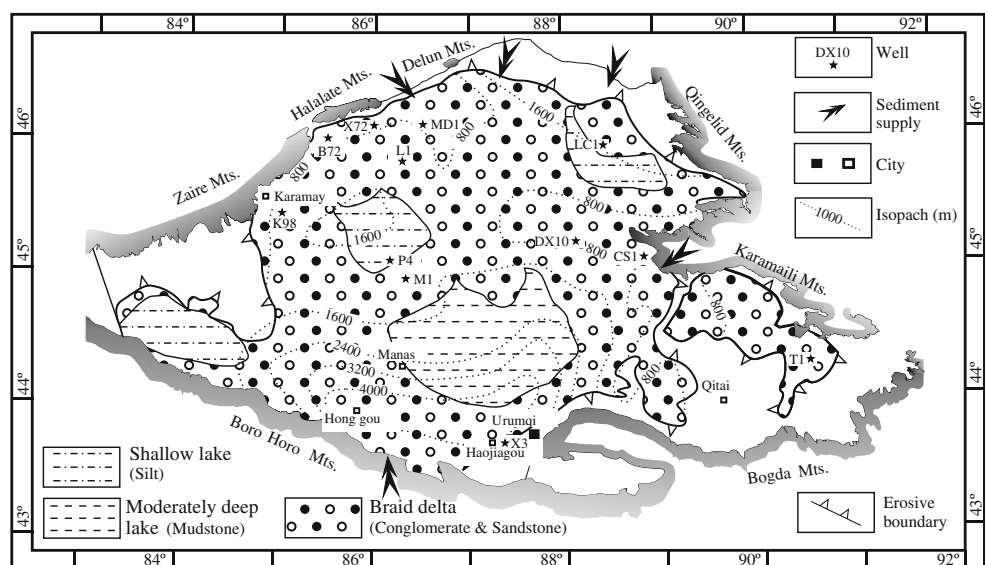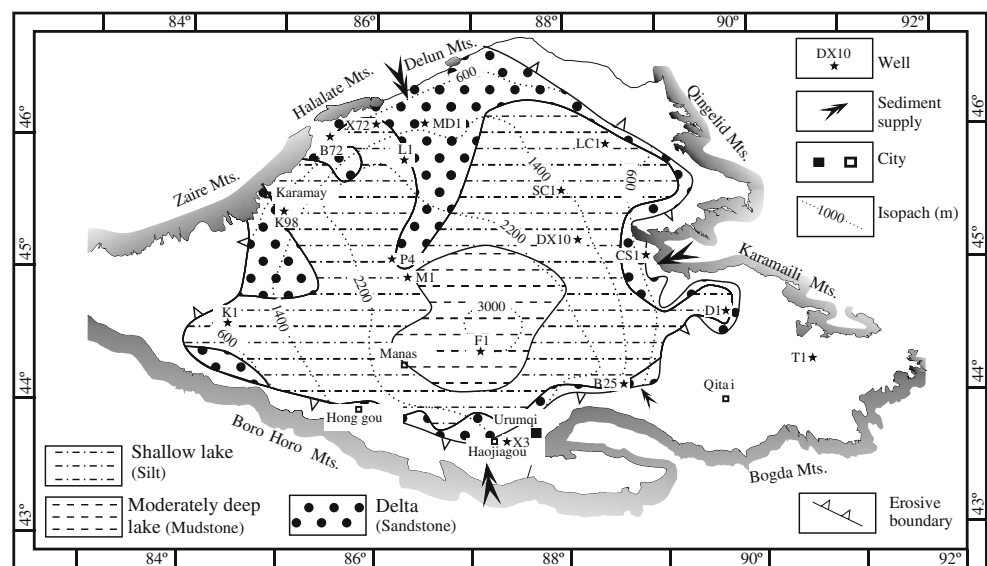
Fig. 7 Lithofacies distribution in the Junggar Basin during the Early Cretaceous (modified after Gu et al. 2003; Zhang et al. 1993) and isopach map for the whole Cretaceous (K) (modified after Tian 1989)

deposits accumulated in braid-delta systems. Throughout the Cretaceous, the depocentre migrated from the southern margin to the basin centre. Here, the maximum thickness of Cretaceous deposits is more than 3,000 m (Fig. 7).

The Palaeogene sedimentary pattern was largely inherited from the Cretaceous. A braid-delta system developed basinwide (Gao et al. 2009). The deposits of two shallow lakes are preserved near the city of Manas and adjacent to the Qingelid Mountains, respectively (Fig. 8). The depocentre located near Manas displays a maximum sedimentary thickness of 1,500 m. Input of clastics was from all sides of the basin.

Reactivated foreland basin cycle (Neogene to Quaternary)

Triggered by the India–Asia collision, the ancient foreland basin in front of the Tian Shan was reactivated and again established a strongly asymmetric depositional architecture within the Junggar Basin with sedimentation restricted to the southern part. Here, Neogene sediment thickness reaches more than 5,000 m rapidly thinning out to the north. Sediment supply was not only from the rising Tian Shan but also from the northern ranges, developing a fan delta system around a central endorheic shallow lake (Fig. 9).

Fig. 8 Lithofacies distribution and isopach map of the Junggar Basin during the Palaeogene (modified after Gu et al. 2003; Zhang et al. 1993)
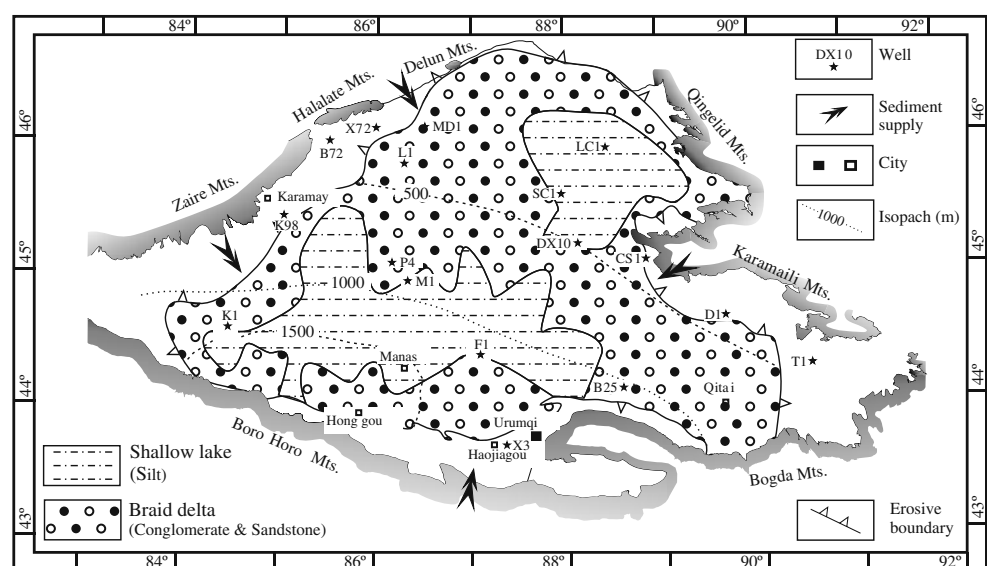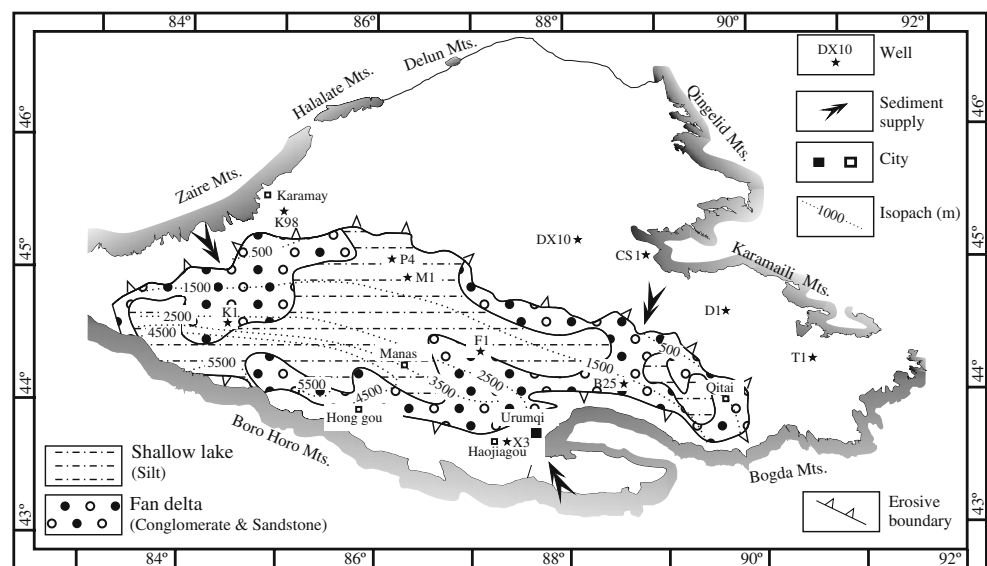
Fig. 9 Lithofacies distribution in the Junggar Basin during the Early Pliocene (Shawan Formation) and isopach map of the Neogene and Quaternary (modified after Zhang et al. 1999b)

Basin evolution and palaeoclimate

Ongoing subsidence with an almost complete Mesozoic–Cenozoic continental sedimentary record, internal drainage together with a relatively permanent latitudinal position between ca. 40 and 50 °N makes the Junggar Basin an excellent recorder of long-term environmental and climatic changes at the southeastern edge of the Asian continent. During this long time span, the Asian continent grew successively to the south by accretion of continental blocks and latest by the collision of the Indian subcontinent, increasingly isolating the Junggar Basin and causing an overall trend of increased continentality and aridity of the climate. This goes along with a break-down of the Pangean megamonsoon during the mid-Mesozoic, and a shift to western and northern sources of humidity by the westerlies (Parrish and Curtis 1982; Hendrix et al. 1992; Carroll et al. 2010).

The overall aridization trend in the Junggar Basin and the cut-off from monsoonal circulation patterns due to plate accretion in the south was strengthened by two processes. First, the westerlies which dominated since the late Mesozoic and became successively less humid in the Palaeogene and Neogene, because marine regression took place over large parts of the Parathethyian realm to the west of which the Caspian Sea is the last remnant nowadays. Second, repeated uplift of the mountain ranges wrapping the Junggar Basin (and also other basins in western China) converted it into a "walled basin", which became geomorphologically isolated while local rainshadows increasingly prevented moisture transfer from outside the basin (Carroll et al. 2010).

The details of this overall palaeoclimatic pattern are not well known to date. Hendrix et al. (1992) and Hendrix

(2000) concluded that the Pangean megamonsoon broke down in the Late Jurassic and a rainshadow established from the physiographically rising Tian Shan in response of the collision of the Lhasa Block in the south. Taking sediment facies, they assigned a humid source in the north, causing deposition of greyish mudstones in the southern Junggar Basin and reddish mudstones in the northern Tarim Basin on the dry side of the orographic barrier. Other examples of climate-sensitive sedimentary facies types are coal deposits, usually interpreted as reflecting peak humidity, iron-rich beds indicating humid conditions and strong chemical weathering, and pedogenetic crusts (calcretes, gypcretes) indicating semiarid conditions. These sedimentological criteria well document increasing aridization since the Middle Jurassic as demonstrated by Ashraf et al. 2010, this issue. However, there are some problems related to rely on sedimentological criteria alone, because, e.g., coal swamps may also develop under a semiarid climate if large riparian areas in a lake shore environment are available (Carroll et al. 2010). In addition, sandstone petrology also fails to detect climate evolution, but well reflects different source areas and tectonic evolution of the Junggar and Tarim Basin (Hendrix 2000; Greene et al. 2005).

To tackle this problem, high resolution palaeobotanical and palynological studies are most promising because of generally good preservation in lacustrine deposits as shown by Ashraf et al. (2010), Hinz et al. (2010) and Sun et al. (2010) (all this issue). High-resolution palynological studies show that besides the overall aridization trend, several fluctuations in humidity can be identified. After a semiarid to subhumid Late Permian with a balanced-filled lake (Fig. 4; Carroll et al. 2010), the Early Triassic was drier and semiarid. During the Late Triassic and Early Jurassic,

humidity reached a maximum. This is in line with the deepening and spreading of the large overfilled freshwater lake and retrogradation of deltaic and fluvial sedimentary facies (e.g., Hornung and Hinderer 2010; Fig. 5). The strong progradation of coarse-grained sediments at the Triassic/Jurassic boundary (Fig. 6) is independent from any climatic signal according to the pollen record, thus supporting the conclusion of a short-term tectonic episode with much increased sediment supply instead of a climate-induced lowering of the lake level.

Following Ashraf et al. (2010, this issue), seasonality increased in the Middle and Late Jurassic and the dry season became more and more dominant. Nevertheless, the lake kept overfilled during most of the Jurassic. The climax of coal deposition appears to be at the beginning of this trend, supporting the hypothesis of Carroll et al. (2010) that coal formation is not identical with highest lake levels but with the establishment of vast flooding areas around the lake. Up to the present, similar high-resolution palynological and palaeobotanical studies are lacking for the Cretaceous and Palaeogene. Such an approach might be hampered by dominantly oxygenized sedimentary facies and a retreat of lacustrine environments (closed lakes), indicating further aridization.

The tectonic as well as palaeoenvironmental evolution of the Junggar Basin is well reflected by similar trends in basins across western China, although basement characteristics and basin forming mechanisms may differ (Carroll et al. 2010; Zhao et al. 2010). Nevertheless, palaeoclimate data of Chinese nonmarine sedimentary basins are still sparse, and a relatively weak biostratigraphic control of lithostratigraphic units as well as the lack of cyclostratigraphic and sequence stratigraphic analysis prevents high-resolution correlation of both, palaeoclimate and tectonic episodes among different basins. For further studies, sedimentary facies, cyclostratigraphy and palaeobotanical studies should be closely combined to elucidate local versus regional palaeoenvironmental patterns and far-distance tectonic forcing.

References

Allen MB, Sengör AM, Natal'in BA (1995) Junggar, Turfan and Alakol Basins as Late Permian to Early Triassic extensional structures in a sinistral shear zone in the Altaid orogenic collage, Central Asia. J Geol Soc Lond 152:327–338

Ashraf AR, Sun Y-W, Sun G, Uhl D, Mosbrugger V, Li J, Herrmann M (2010) Triassic and Jurassic palaeoclimate development in the Junggar Basin, Xinjiang, Northwest China - a review and additional lithological data. In: Martin T, Sun G, Mosbrugger V (eds) Triassic-Jurassic biodiversity, ecosystems, and climate in the Junggar Basin, Xinjiang, Northwest China. Palaeobio Palaeoenv 90(3). doi:10.1007/s12549-010-0034-0

Busby CJ, Ingersoll RV (eds) (1995) Tectonics of sedimentary basins. Blackwell, Oxford

Carroll AR, Liang Y-H, Graham SA, Xiao X-C, Hendrix MS, Chu JC, Mcknight CL (1990) Junggar Basin, Northwest China: trapped Late Paleozoic ocean. Tectonophysics 181:1–14

Carroll AR, Brassell AR, Graham SA (1992) Upper Permian lacustrine oil shales of the southern Junggar Basin, Northwest China. Am Assoc Pet Geol Bull 76:1874–1902

Carroll AR, Graham SA, Hendrix MS, Ying D, Zhou D (1995) Late Paleozoic tectonic amalgamation of northwestern China: Sedimentary record of the northern Tarim, northwestern Turpan, and southern Junggar Basins. Geol Soc Am Bull 107:571–594

Carroll AR, Graham SA, Smith, ME (2010) Walled sedimentary basins of China. In: Graham SA, Carroll AR, Ping L (eds) Tectonic and stratigraphic evolution of nonmarine basins of China. Basin Res 22:17–32

Chen X, Lu H-F, Shu L-S, Wang H-M, Zhang G-Q (2002) Study on tectonic evolution of Junggar Basin. Geol J China Univ (03):257–267 (in Chinese with English abstract)

De Grave J, Buslov MM, Van den Haute P (2007) Distant effects of India-Eurasia convergence and Mesozoic intracontinental deformation in central Asia: constraints from apatite fission-track thermochronology. J Asian Earth Sci 29:188–204

Dickinson WR, Snyder WS (1978) Plate tectonics of the laramide orogeny. Geol Soc Am Mem 151:355–366

Ding A-N, Hui R-Y, Meng X-Q (1996) Characteristics of source rocks and their hydrocarbon formation in Jurassic system, Junggar Basin, Xinjiang. Petro Explor Develop 23:11–18 (in Chinese with English abstract)

Fang S-H, Guo Z-J, Wu C-D, Zhang Z-C, Wang M-N, Yuan Q-D (2006) Jurassic clastic composition in the southern Junggar Basin, northwest China: Implications for basin-range pattern and tectonic attributes. Acta Geol Sin 80:196–209 (in Chinese with English abstract)

Feng J-W, Dai J-S, Ge S-Q (2008) Structural evolution and pool-forming in Wuxia fault belt of Junggar Basin. J China Univ Petro (Nat Sci) 32:23–29 (in Chinese with English abstract)

Gao L, Zhu X-M, Lü X-Y (2004) Sedimentary facies of lower Cretaceous in Sangequan area of Junggar Basin. J Univ Petro China 28:5–9 (in Chinese with English abstract)

Gao Z-Y, Han G-M, Zhu R-K, Guo H-L, Wang D-C, Li B-L (2009) Depositional setting and evolution of the Paleogene-Neogene foreland basin of southern margin of Junggar Basin. J Palaeogeogr 11:491–502 (in Chinese with English abstract)

Graham SA, Hendrix MS, Wang L-B, Carroll AR (1993) Collisional successor basins of western China - impact of tectonic inheritance on sand composition. Geol Soc Am Bull 105:323–344

Greene TJ, Carroll AR, Wartes M, Graham SA (2005) Integrated provenance analysis of a complex orogenic terrane: Turpan-Hami Basin, NW China. J Sediment Res 75:251–267

Gu Y-F, Ma M-F, Su S-L, Min X-H, Hu B, Yao W-J (2003) Lithofacies paleogeography of the Cretaceous in the Junggar Basin. Petro Geol Exp 25:337–342 (in Chinese with English abstract)

Guo B, Liu Q-Y, Chen J-H, Zhao D-P, Li S-C, Lai Y-G (2006) Seismic tomography of the crust and upper mantle structure underneath the Chinese Tianshan. Chin J Geophy 49:1693–1700 (in Chinese with English abstract)

Han B-F, He G-Q, Wang S-G (1999) Postcollisional mantle-derived magmatism, underplating and implication for basement of the Junggar Basin. Sci China Ser D 42:113–119

He Z-P, Shao L-Y, Kang Y-S, Liu Y-F, Luo W-L, Feng Q-X (2004) Analysis on controls of the coal accumulation in the Jurassic Badaowan formation, Junggar Basin. Acta Sediment Sinica 22:449–454 (in Chinese with English abstract)

He D-F, Zhai G-M, Kuang J, Zhang Y-J, Shi Y (2005) Distribution and tectonic features of paleo-uplifts in the Junggar Basin. Chin J Geol 40:248–261 (in Chinese with English abstract)

Hendrix MS (2000) Evolution of Mesozoic sandstone compositions, southern Junggar, northern Tarim, and western Turpan Basins, northwest China: A detrital record of the ancestral Tian Shan. J Sed Res 70:520–532

Hendrix MS, Graham SA, Carroll AR, Sobel ER, Mcknight CL, Schulein BJ, Wang Z (1992) Sedimentary record and climatic implications of recurrent deformation in the Tian Shan: evidence from Mesozoic strata of the north Tarim, south Junggar, and Turpan Basins, northwest China. Geol Soc Am Bull 104:53–79

Hendrix MS, Dumitru TA, Graham SA (1994) Late Oligocene-early Miocene unroofing in the Chinese Tian Shan: an early effect of the India-Asia collision. Geology 22:487–490

Hinz JK, Smith I, Pretzschner H-U, Wings O, Sun G (2010) A high-resolution three-dimensional reconstruction of a fossil forest (Upper Jurassic Shishugou Formation, Junggar Basin, Northwest China). In: Martin T, Sun G, Mosbrugger V (eds) Triassic-Jurassic biodiversity, ecosystems, and climate in the Junggar Basin, Xinjiang, Northwest China. Palaeobio Palaeoenv 90(3) doi:10.1007/s12549-010-0036-y

Hornung J, Hinderer M (2010) Depositional dynamics and preservation potential in a progradational lacustrine to fluvial setting: Implications for high resolution sequence stratigraphy (Upper Triassic, NW-China). SEPM Spec Publ River to Rockrecord (in press)

Hu A-Q, Wang Z-G, Tu G-C (1997) Geological evolution, diagenesis and metallogeny of the northern Xinjing. China Science Press, Beijing

Hu Z-Q, Zhu X-M, Peng Y-M (2001) Analysis of provenance and palaeocurrent direction of Jurassic at Chepaizi region in northwest edge of Junggar Basin. J Palaeogeogr 3:49–54 (in Chinese with English abstract)

Huang Z-Y (1999) Sedimentary facies and their bearings on oil and gas accumulation in the lower Permian Jiamuhe formation along the northwestern margin of the Junggar Basin, Xinjiang. Sediment Facies Palaeogeogr 19:38–46 (in Chinese with English abstract)

Kang Y-Z (2008) Characteristics of the Carboniferous-Permian volcanic rocks and hydrocarbon accumulations in two great basins, Xinjiang area. Petro Geol Exp 30:321–327 (in Chinese with English abstract)

Kuang J, Qi X (2006) The Structural Characteristics and Oil-Gas Explorative Direction in Junggar Foreland Basin. Xinjiang Petro Geol 27:5–9 (in Chinese with English abstract)

Kuang L-C, Lu H-T, Xue J-J, Zhu X-M, Li D-J (2008) Characteristics of volcanic reservoirs in Jiamuhe formation of Permian in the 5th and 8th districts, northwestern margin of Junggar Basin. Geol J China Univ 14:164–171 (in Chinese with English abstract)

Lawrence SR (1990) Aspects of petroleum geology of the Junggar Basin, northwest China. In Brooks J (ed) Classic Petroleum Provinces. Geol Soc London Spec Publ 50:545–557

Li W, Hu J-M, Qu H-J (2009) Discussion on Mesozoic basin boundary of the northern Junggar Basin, Xinjiang. J Northwest Univ (Nat Sci) 39:820–821 (in Chinese with English abstract)

Liu W-B (1989) Study on sedimentary environment of Fengcheng formation at northwest margin of Junggar Basin. Acta Sediment Sinica 7:61–70 (in Chinese with English abstract)

Liu C-H, Peng Y-M, Xiang K, Ma L-Q (2006) Sequence stratigraphy and subtle-trap identification in the hinterland of Junggar Basin. Geological Publishing House, Beijing

Liu J-Z, Zhang S-F, Guan J, Zhao W-J (2008) Sedimentary characteristics of Jurassic fan-delta in Chepaizi area, northwest margin of Junggar Basin. Spec Oil Gas Reserv 15:27–30 (in Chinese with English abstract)

Luo X-R, Liu L-J, Li X-Y (2006) Overpressure distribution and pressuring mechanism on the southern margin of the Junggar Basin, Northwestern China. Chin Sci Bull 51:2383–2390

Luo Z-J, Wang R, Zhao J-H A L-Y (2007) Late Permian-middle Jurassic megaspores assemblages in the north-west area, Junggar Basin. Xinjiang Geol 25:243–247 (in Chinese with English abstract)

Metcalfe I, Foster CB, Afonin SA, Nicoll RS, Mundil R, Wang X-F, Lucas SG (2009) Stratigraphy, biostratigraphy and C-isotopes of the Permian-Triassic non-marine sequence at Dalongkou and Lucaogou, Xinjiang Province, China. J Asian Earth Sci 36:503–520

Mou Z-H, Zhu D-Y, Qing C-W (1992) Sedimentary facies and patterns of Carboniferous and Permian in Junggar Basin. Xinjiang Petro Geol 13:35–48 (in Chinese with English abstract)

Parrish JT, Curtis RL (1982) Atmospheric circulation, upwelling, and organic-rich rocks in the Mesozoic and Cenozoic eras. Palaeogeogr Palaeoclimatol Palaeoecol 40:31–66

Qu G-S, Ma Z-J, Shao X-Z, Zhang X-K (2008) Basements and crust structures in Junggar Basin. Xinjiang Petro Geol 29:669–674 (in Chinese with English abstract)

Sengör AMC, Natal'In BA, Burtman VS (1993) Evolution of the Altaid tectonic collage and Palaeozoic crustal growth in Eurasia. Nature 364:299–307

Shao L, Stattegger K, Wenhou L, Haupt BJ (1999) Depositional style and subsidence history of the Turpan Basin (NW China). Sediment Geol 128:155–169

Shao L, Stattegger K, Garbe-Schoenberg CD (2001) Sandstone petrology and geochemistry of the Turpan Basin (NW China): Implications for the tectonic evolution of a continental basin. J Sediment Res 71:37–49

Sobel, ER, Hilley GE, Strecker MR (2003) Formation of internally-drained contractional basins by aridity-limited bedrock incision. J Geophys Res 108(B7), 2344. doi:10.1029/2002JB001883

Song C-C (2006) Sedimentary system and sedimentary features of central Junggar Basin. Geological Publishing House, Beijing

Sun G, Mosbrugger V, Miao Y-Y, Ashraf AR (2010) The Upper Triassic to Middle Jurassic strata and floras of the Junggar Basin, Xinjiang, Northwest China. In: Martin T, Sun G, Mosbrugger V (eds) Triassic-Jurassic biodiversity, ecosystems, and climate in the Junggar Basin, Xinjiang, Northwest China. Palaeobio Palaeoenv 90(3) doi:10.1007/s12549-010-0039-8

Tang Z-H, Parnell J, Longstaffe FJ (1997) Diagenesis and reservoir potential of Permian-Triassic fluvial/lacustrine sandstones in the southern Junggar Basin, northwestern China. AAPG Bull 81:1843–1865

Tian Z-Y (1989) The analysis of oil and gas prospect in Junggar basin from geological developmental history. Xinjiang Petro Geol 03:3–14 (in Chinese with English abstract)

Wang Y-L, Wang Y-M, Qi X-F, Guan S-R, Zhao X-Q, Li R-F (2001) Classification of stratigraphic sequences of Jurassic in Junggar basin. Xinjiang Petro Geol 22:382–385 (in Chinese with English abstract)

Wang M-F, Jiao Y-Q, Ren J-Y, Tong D-J, Xu Z-C (2007) Characteristics of Jurassic subsidence and its relation with tectonic evolution in Junggar Basin. Acta Petr Sinica 28:27–32 (in Chinese with English abstract)

Wang B, Cluzel D, Shu L, Faure M, Charvet J, Chen Y, Meffre S, de Jong K (2009) Evolution of calc-alkaline to alkaline magmatism through Carboniferous convergence to Permian transcurrent tectonics, western Chinese Tianshan. In: Xiao W, Kröner A, Windley, BF (eds) Geodynamic evolution of Central Asia in the Paleozoic and Mesozoic. Int J Earth Sci 98:1275–1298

Wu X-Q, Liu D-L, Wei G-Q, Li J, Li Z-S (2009) Geochemical characteristics and tectonic settings of Carboniferous volcanic rocks from Ludong-Wucaiwan area, Junggar Basin. Acta Petr Sinica 25:55–66 (in Chinese with English abstract)

Xiao W-J, Windley B-F, Huang B-C, Han C-M, Yuan C, Chen H-L, Sun M, Sun S, Li J-L (2009) End-Permian to mid-Triassic termination of the accretionary processes of the southern Altaids: implications for the geodynamic evolution, Phanerozoic continental growth, and metallogeny of Central Asia. In: Xiao W, Kröner A, Windley, BF (eds) Geodynamic evolution of Central Asia in the Paleozoic and Mesozoic. Int J Earth Sci 98:1189–1217

Xu X-K, Shen Y, Zhao H-L, Zhuang X-M, Li J (2004) Hydrocarbon accumulation regulation and exploration prospect in Junggar Basin. In: Liu G-D, Jia C-Z (eds) Oil exploration in Junggar Basin: Symposia of Chinese geophysical society workshop about oil exploration in Junggar Basin. Petroleum Industry Press, Beijing, pp 23–46

Yan J-H, Chen S-Y, Cui Y-B, Liu Z-Y (2009) Sedimentary features and favorable reservoirs of Permian in Wu-Xia area of Junggar Basin. Xinjiang Petro Geol 30:304–306 (in Chinese with English abstract)

Yang J-L, Wang Q-F, Lu H-N (2005) Discovery of Cretaceous and Paleocene charophyte floras from well Hu-2 in the southern edge of Junggar Basin. Acta Micropalaeontol Sinica 22:251–268 (in Chinese with English abstract)

Yang J-L, Wang Q-F, Lu H-N (2008) Cretaceous charophyte floras from the Junggar basin, Xinjiang, China. Acta Micropalaeontol Sinica 25:345–363 (in Chinese with English abstract)

Yang T-N, Li J-Y, Wang Y, Dang Y-X (2009) Late Early Permian (266 Ma) N-S compressional deformation of the Turfan basin, NW China: the cause in the change of basin pattern. In: Xiao W, Kröner A, Windley, BF (eds) Geodynamic evolution of Central Asia in the Paleozoic and Mesozoic. Int J Earth Sci 98: 1311–1324

Yu Y-J, Hu S-Y, Lei Z-Y, He D-F, Zhang L-P, Xu S-J (2005) Sedimentary response to Triassic-Jurassic thrust faulting in the foreland thrust belt of the northwestern Junggar Basin. Earth Sci Front 12:423–436 (in Chinese with English abstract)

Zhang G-J, Wang Z-H, Wu M, Wu Q-F, Yang B, Yang W-X, Yang R-L, Fan G-H, Zheng D-S, Zhao B, Peng X-L, Yong T-S (1993) Xinjiang, Junggar basin. Petroleum Industry Press, Beijing

Zhang G-C, Chen X-F, Liu L-J, Yu L-P, Wang Z (1999a) The tectonic evolution, architecture and petroleum distribution in the Zhungaer basin in China. Acta Petr Sinica 20:21–26 (in Chinese with English abstract)

Zhang Y-J, Wang H-M, He Z-H (1999b) The basement structure, the formation and the evolution of Junggar Basin. Xinjiang Petro Geol 20:568–571 (in Chinese with English abstract)

Zhang J-S, Hong D-W, Wang T (2004) Geophysical researches on the basement properties of the Junggar Basin. Acta Geosci Sinica 25:473–478 (in Chinese with English abstract)

Zhao J-M, Huang Y, Ma Z-J, Shao X-Z, Cheng H-G, Wang W, Xu Q (2008) Discussion on the basement structure and property of northern Junggar Basin. Chin J Geophy 51:1767–1775 (in Chinese with English abstract)

Zhao W, Wang H, Yuan X, Wang Z, Zhu G (2010) Petroleum systems of Chinese nonmarine basins. In: Graham SA, Carroll AR, Ping L (eds) Tectonic and stratigraphic evolution of nonmarine basins of China. Basin Res 22:4–16

Zhu X-M, Kang A, Zhang Q, Zhang M-L, Kuang J, Wu X-Z, Han J (2002) Sequence stratigraphy of Jurrasic coal - bearing measure and subtle trap in the northeast edge of Junggar Basin. Oil Gas Geol 23:121–126 (in Chinese with English abstract)

Zhu X-M, Zhang Y-N, Yang J-S, Li D-J, Zhang N-F (2008) Sedimentary characteristics of the shallow Jurassic braided river delta, the Junggar Basin. Oil Gas Geol 29:244–251 (in Chinese with English abstract)

Zou C-N, Hou L-H, Kuang L-C, Kuang J (2007) Genetic mechanism of diagenesis-reservoir facies of the fan-controlled Permo-Triassic in the western marginal area, Junggar Basin. Chin J Geol 42:587–601 (in Chinese with English abstract)